Study of Ambient Light Impact on RSS-Based Indoor Positioning System Using Visible Light Communication

Ameur Chaabna[1], **Abdesselam Babouri**[2†], **Xun Zhang**[3], **Fayçal Boulsina**[4], and **Takoua Hafsi**[5], Non-members

ABSTRACT

An optical wireless positioning system that uses white light-emitting diodes (LEDs) based on Visible Light Communication (VLC) is presented in this paper. In the proposed system, four LEDs are employed for illumination and communication. The trilateration technique is used for determining the receiver's location and the practical Received Signal Strength (RSS) measurements are used for distance estimation. The impact of ambient light on Signal-to-Noise-Ratio (SNR) is studied by taking into consideration the first-order light reflection off of the ceiling, floor, and walls for channel modeling with both direct and indirect sunlight exposure. A modeling equation from the RSS measurements is proposed. The results show that the illuminance in all of the places in the room can be satisfied. Furthermore, the average positioning error by adopting the derived equation and trilateration technique was an error of less than 3 cm.

Keywords: Visible Light Communication (VLC), Indoor Positioning System (IPS), Light-emitting Diode (LED), Trilateration, Received Signal Strength (RSS)

1. INTRODUCTION

In many applications there is a need to locate people or objects. That is why localization, or positioning, is a major research area. There are two categories of positioning systems: Outdoor and Indoor. For Outdoor Positioning systems, there are several systems such as the Global Positioning System (GPS), the Global Navigation Satellite System (GNSS), and the BeiDou Navigation Satellite System (BDS). Due to the influence of multi-path or radio disturbance inside buildings, it is hard for these systems to provide an accurate location in an indoor environment [1]. Hence, many methods to achieve Indoor Positioning have been proposed. Some of them are based on infrared light or ultrasonic waves, Radio-Frequency Identification (RFID), Ultra-Wide Band (UWB), Bluetooth, ZigBee, and Wi-Fi. They tend to have a large error in distance ranging from centimeters to meters [2]. Others are based on location networks. In [3] the authors proposed an algorithm for estimation of position of a target in a mobile network. In this algorithm, every node selects a subset of its neighbors that satisfy a given threshold.

Recently, the VLC-based Indoor Positioning System (VLC-IPS) is receiving attention because it is more accurate and well-equipped infrastructure exists even for future 5G and beyond 5G location based service [4]. In Wireless Indoor Positioning Systems (IPS), there are mainly three mathematical techniques used by their algorithms: Proximity, Triangulation, and Scene Analysis [5]. Triangulation is based on the knowledge of geometric properties of triangles to determine the target location. It consists of two branches: Lateration and Angulation.

The trilateration technique used in this paper determines the target location by measuring its distance from multiple points with known coordinates called reference points. This distance is measured indirectly by using several different approaches: Time Of Arrival (TOA), Received Signal Strength (RSS), and Time Difference Of Arrival (TDOA) or Roundtrip Time Of Flight (RTOF) [6].

Using white LEDs on the transmitter's side is the best way to provide high speed communications as well as general illumination [7, 8]. The authors in [9] considered all of the optical channels LOS. A new

Manuscript received on May 23, 2019 ; revised on June 7, 2020 ; accepted on June 22, 2020. This paper was recommended by Associate Editor Piya Kovintavewat.

[1]The author is with the LABCAV Laboratory, Department of Electronics and Telecommunications, Université 8 Mai 1945 Guelma, Algeria.

[2]The author is with the LGEG Laboratory, Department of Electrical and Automatic Engineering, Université 8 Mai 1945 Guelma, Algeria.

[3]The author is with the MINARC Laboratory, Department of Electronic and Computer Engineering, Institut Supérieur d'Électronique de Paris, France.

[4]The author is with the LHS Laboratory Constantine 1, Department of Electronics and Telecommunications, Université 8 Mai 1945 Guelma, Algeria.

[5]The author is with the LAM2SIN Laboratory, Department of Mathematics, Université Badji Mokhtar - Annaba, Algeria.

[†]Corresponding author: abdesselam.babouri@gmail.com

Digital Object Identifier 10.37936/ecti-eec.2021191.226818

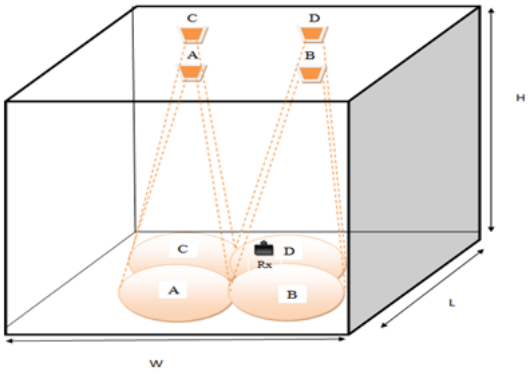

Fig.1: *Model of the room.*

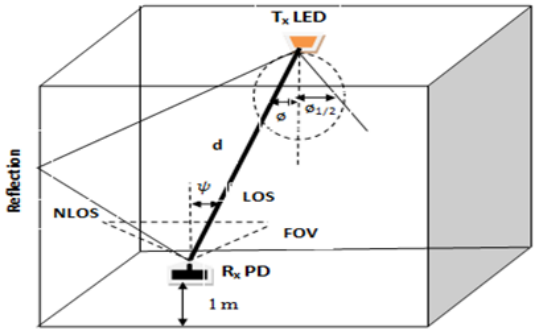

Fig.2: *LOS and NLOS optical wireless channel model.*

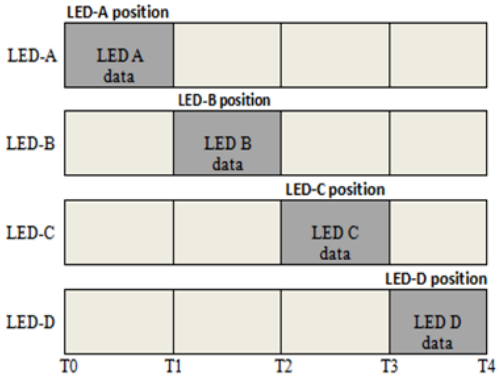

Fig.3: *The TDM protocol for an IPS comprising 4 LEDs using OOK.*

method by selecting communicating LEDs (C-LEDs) to optimize the SNR is proposed in [10]. In [5], an algorithm able to provide positioning resolution higher than 0.5 mm is proposed. The researchers in [11] outline several approaches with data rates equal to or greater than 100 Mb/s.

Generally, there are two categories of optical receiver: photodiode and solar cell [12]. In this work a Bpw34 photodiode is used. The receiver collects hybrid light composed by direct and reflected light. As it is known that the rate of direct light is about 95%, the first reflected light is 3.57%, and the second reflected light is 1.27%.

In this paper, a VLC-based Indoor Positioning System (VLC-IPS) using a trilateration technique and RSS information is proposed. The localization accuracy in different ambient light scenarios is compared. Different indoor illumination and SNR distributions are evaluated in our simulation by considering the first-order light reflection at each wall, as well as direct and indirect sunlight exposure. Those scenarios are illustrated by a mixed optical wireless channel model, which was studied in research about wireless infrared communication [13, 14]. The researchers analyze the performance and present the benefits of partial pre-equalization for indoor optical wireless transmissions based on asymmetrically clipped optical orthogonal frequency division multiplexing (ACO-OFDM) with intensity modulation and direct detection (IM/DD). In those papers some parameters are not studied, Bit-Error-Rate (BER) performance is presented in [15]. Reference points of the model are the light sources and the target is the optical receiver. The simulation of the model was carried out using MATLAB software.

The remainder of this paper is organized as follows: In Section 2 the optical channel and the positioning algorithm are described. In Section 3 the results of illuminance performance, the SNR, and the different estimated positions are presented. Finally, a conclusion is drawn in Section 4.

2. MODELLING OF PROPOSED SYSTEM

2.1 Optical Wireless Channel Model

The overview of the proposed indoor localization system employing LED ceiling lamps is depicted in Fig. 1. The four LEDs used here are identical and they are white.

It is assumed that the source of emission and the reflected points on wall have a Lambertian radiation pattern [16]. The light beams from the LEDs to the receiver are propagated via two main types of channels: Line-Of-Sight (LOS) channels and Non Line-Of-Sight (NLOS) channels, which are illustrated in Fig. 2.

In this design, all LEDs function as lamps for light all of the time. To resolve the problem that the receiver receives multiple ID data from different transmitters at the same time, each LED should transmit ID data at different times. Hence, the transmission time is divided into frames. Each one of the LEDs is divided into several time intervals, as shown in Fig. 3. This allows the receiver to distinguish between the different received signals. Thus, the Time Division Multiplexing (TDM) protocol is essential for transmission.

Each receiver can only receive data for one ID during each slot time according to the data transmission protocol [22] described next.

Encoding mode: The positioning system plays a role in the lighting when estimating the location of the target receiver. When the condition of continuous "0" or "1" values in the data occurs, our eyes may feel the light is twinkling. To avoid this state, we chose the Manchester encoding to encode the data transmitted by the LEDs. In the Manchester encoding, signal "0" is encoded into "01" and the signal "1" is encoded into "10". So whatever the original data is, the coded data is consisted by the alternate "0" and "1" and the function of lighting will never be affected even in a worse case situation.

Frame structure: In order to make it possible for the receiver to identify the data transmitted by the LEDs, we design the frame structure based on Manchester encoding. In the data frame, "1111" represents the frame head and "0000" the end of the frame. The reason that we use these two elements is that "00" and "11" are illegal sequences in Manchester encoding rules, and "1111" and "0000" never appear in the consecutive codes of properly encoded data. In the frame, the positioning ID data, whose length is 8 bits, is between "1111" and "0000". The first 4 bits represent the X coordinate and the latter 4 bits represent the Y coordinate in the 2-D plane. After being encoded, the length of the data is 16 bits. Thus the length of a frame is 24 bits. In this positioning system, we set the time slot as 1 ms and thus the required data rate for ID data transmission is 24 kbps.

The local location is confirmed by using the change in signal features which depend on the distance and the angle between the transmitter and the receiver [2].

2.1.1 Description of optical wireless LOS channel

According to [16], the LOS channel links are characterized by the DC gain. Generally, the Optical Wireless Channel (OWC) receivers employ optical filters to attenuate ambient light and use concentrators to increase effective light-collection area. The channel DC gain is given by

$$H(0)_{LOS} = \begin{cases} \frac{m+1}{2\pi d^2} A \cos^m(\phi) \cos(\psi), & 0 \le \psi \le \psi_c \\ 0, & \psi > \psi_c \end{cases} \quad (1)$$

where A is the photodiode active area, ψ is the angle of incidence with respect to the receiver axis, ψ_c is the Field Of View (FOV) of detector, ϕ is the angle of irradiance with respect to the transmitter perpendicular axis, and d is the distance between transmitter and receiver. The Lambertian order m is given by $m = -\ln 2 / \ln\left(\cos\phi_{1/2}\right)$, where $\cos\phi_{1/2}$ is the half power angle of the LED bulb. The total optical power of i LEDs is given by

$$P_{rx,LOS} = \sum_{i=1}^{LEDs} P_{tx} H^i_{LOS}(0) \quad (2)$$

where $H^i_{LOS}(0)$ is i^{th} LED channel DC gain, and P_{tx} is the transmitted optical power from LED.

2.1.2 Description of optical wireless NLOS channel

For the optical wireless NLOS signal modeling, we follow the same method used for the sphere model [13]. In a room, over the whole surface S_{room}, an intensity I_1 is emitted by the first diffuse reflection of a wide-beam optical source which is given by

$$I_1 = \rho_1 \frac{P_{totalLED}}{S_{room}} \quad (3)$$

where ρ_1 is the reflectivity of the surface and $P_{totalLED}$ is the total power of all the LEDs.

The average reflectivity $< \rho >$ is defined in Eq. (4)

$$< \rho >= \frac{1}{S_{room}} \sum_i S_i \rho_i \quad (4)$$

where $< \rho >$ is the individual reflectivity of walls, ceiling, floor, and other objects in the room which are weighted by their individual areas S_i.

The total intensity is given by summing up the geometrical series in Eq. (5).

$$I = I_1 \sum_{j=1}^{\infty} < \rho >^{j-1} = \frac{I_1}{1 - < \rho >} \quad (5)$$

where j is the number of reflections.

The receiver is assumed as a small part of the room surface, so the received NLOS power P_{NLOS} with the receiving area S_{rx} is given by

$$P_{NLOS} = S_{rx} I \quad (6)$$

The NLOS channel loss is given by

$$\eta_{NLOS} = \frac{P_{NLOS}}{P_{totalLED}} = \frac{S_{rx}}{S_{room}} \frac{\rho_1}{1 - < \rho >} \quad (7)$$

2.1.3 Superposition of LOS and NLOS channels

The received power is given by

$$P_{rx} = (P_{LOS} + P_{NLOS}) * T_s(\psi) * g(\psi) \quad (8)$$

where $T_s(\psi)$ is the gain of the optical filter, and $g(\psi)$ is the gain of the optical concentrator. The combined channel gain is given by Eq. (9) [13].

$$H_{NLOS+LOS}(f) = H(0)_{LOS} + H_{NLOS}(f) e^{j2\pi f \Delta T} \quad (9)$$

where ΔT describes the delay between the LOS signal and the onset of the NLOS signal.

Table 1: *Parameters of simulation.*

Parameter	Value
Room size (L × W × H)	$6 \times 6 \times 4$ m^3
Constant optical power emitted from LED P_{const}	16 W
Coordinates of each LED	A (2, 2, 4) B (4, 2, 4) C (2, 4, 4) D (4, 4, 4)
Emitted codes for each LED	A (1 0 0 0) B (0 1 0 0) C (0 0 1 0) D (0 0 0 1)
Modulation depth η_{OOK}	0.125
Receiver height	1 m
T_k	295 k
G_0	10
η	112 pF/cm^2
I_2	0.562
k	1.38066×10^{-23}
Γ	1.5
g_m	30 ms
I_3	0.0868

The optical concentrator gain $g(\psi)$ is given by Eq. (10) [16].

$$g(\psi) = \begin{cases} \dfrac{\eta_c^2}{\sin^2(\psi_c)}, & 0 \le \psi \le \psi_c \\ 0, & \psi > \psi_c \end{cases} \tag{10}$$

where η_c denotes the refractive index of the concentrator. The parameters used for simulation are summarized in Table 1.

2.2 Illuminance Distribution

Following the function for an optical link [16 – 17], the luminous intensity in angle ϕ is given by

$$I(\phi) = I(0)\cos^m(\phi) \tag{11}$$

where $I(0)$ is the centre luminous intensity of the LEDs. The horizontal illuminance E_{hor} at a point (x, y, z) is given by

$$E_{hor}(x, y, z) = \frac{I(0)\cos^m(\phi)}{d^2\cos(\psi)} \tag{12}$$

The values used for simulation are listed in Table 2.

2.3 SNR Analysis

The Signal-to-Noise-Ratio (SNR) was calculated to examine its effects on the system. The signal component is given by

$$S = (RP_{rx})^2 \tag{13}$$

where R is the detector responsivity (A/W).

Table 2: *Simulation of illuminance.*

Parameter	Value
Semi angle at half power	50°
Reflection coefficient	0.8
Floor reflectivity	0.15
Ceiling reflectivity	0.8
Wall reflectivity	0.7

Table 3: *Receiver parameters.*

Parameter	Value
Field of View (FOV) ψ_c (half angle)	70°
Physical area of photodetector (A)	1.0 cm^2
Gain of optical filter $T_s(\psi)$	1.0
Refractive index of optical concentrator η_c	1.5
Optical/electrical efficiency γ	0.54 (A/W)

Assuming that the noise is Gaussian and is the sum of the shot and thermal noise [18], its total variance σ^2_{total} is given by

$$\sigma^2_{total} = \sigma^2_{shot} + \sigma^2_{thermal} \tag{14}$$

The shot noise variance is given by

$$\sigma^2_{shot} = 2q\gamma(P_{rx})B + 2qI_{bg}I_2B \tag{15}$$

where q is the electronic charge. γ is the optical/electrical (O/E) conversion efficiency. B is the equivalent noise bandwidth which equals here to the modulation bandwidth. I_{bg} is the background current whose traditional value 5100 μA given direct sunlight exposure and 740 μA assuming indirect sunlight exposure [19]. I_2 is the noise bandwidth factor equals to 0.562 [14]. A p-i-n field effect transistor (FET) transimpedance receiver is used and the noise contributions from gate leakage current and 1/f noise are negligible [20].

The thermal noise variance is given by

$$\sigma^2_{thermal} = \frac{8\pi kT_k}{G_0}\eta AI_2B^2 + \frac{16\pi^2kT_k\Gamma}{g_m}\eta^2A^2I_3B^3 \tag{16}$$

The two terms in Eq. (16) are the feedback-resistor noise and the FET channel noise respectively. Here, k is Boltzmann's constant, T_k is the absolute temperature, G_0 is the open-loop voltage gain, η is the fixed capacitance of photo detector per unit area, Γ is the FET channel noise factor, and g_m is the FET transconductance. The receiver parameters used for simulation are listed in Table 3.

2.4 Positioning Algorithm

In this section, our RSS based positioning algorithm will be illustrated. The trilateration technique to estimate the receiver's distance from transmitters on the ceiling and the RSS information of received

signals is used. The LEDs deliver a constant power level in output for illumination purposes. Therefore, only one modulated signal is received by the receiver.

OOK modulation [21] is used to minimize the flickering problem. The modulation depth is 0.125. As each LED emits an optical power proportional to the amplitude of the electrical signal, the resulting power difference on the transmitter side is given by

$$P_{totalLED} = \eta_{OOK} \cdot P_{const} \tag{17}$$

where η_{OOK} is the modulation depth of the OOK modulation. P_{const} is the constant optical power emitted from the LED without using modulation. Therefore, the difference at the receiver side P_{rx} will be given by

$$P_{rx}{=}H_{NLOS+LOS}\,(f) \cdot P_{totalLED} \tag{18}$$

d_{est} is the distance between the transmitter and the receiver and can be estimated by measuring P_{rx} at the receiver [21]

$$d_{est} = \sqrt{\frac{(m{+}1)\,A\cos^m(\phi)T_s(\psi)\,g(\psi)\cos(\psi)P_{totalLED}}{2\pi P_{rx}}} \tag{19}$$

Using geometric properties and assuming that both receiver axis and transmitter axis are perpendicular to the ceiling, we get

$$\cos(\psi) = \cos(\phi) = \frac{H}{d_{est}} \tag{20}$$

The parameter d_{est} is given by

$$d_{est} = \sqrt{d_{est-xy}^2 + H^2} \tag{21}$$

where d_{est-xy} is the estimated horizontal distance between the transmitter and the receiver. H is the vertical distance between the ceiling and the receiver. Through an algebraic simplification, taking into consideration the previous equations, we obtain

$$d_{est-xy} = \sqrt{\frac{(m{+}1)\,A\cos^m(\phi)T_s(\psi)\,g(\psi)\cos(\psi)P_{totalLED}}{2\pi P_{rx}} - H^2} \tag{22}$$

To determine the current position of the receiver in two dimensions (2-D) using trilateration, the signals coming from the four LEDs are needed. Based on the practical measurements, Eq. (23) is derived to estimate the target's distances relative to the referenced LEDs [22].

$$g(\psi) = \begin{cases} \dfrac{A}{d_{est}^2}\cos^m(\phi)\cos(\psi), & 0 \le \psi \le \psi_c \\ 0, & \psi > \psi_c \end{cases} \tag{23}$$

From Eqs. (20), (21) and (23) we can get

$$RSS = \frac{A}{{d_{est-xy}}^2 + H^2} \cdot \left(\frac{H}{\sqrt{{d_{est-xy}}^2 + H^2}}\right)^{m+1} \tag{24}$$

To simplify the analysis, Eq. (24) can be rewritten as

$$\frac{1}{RSS^2} = \alpha.({d_{est-xy}}^2 + H^2)^p \tag{25}$$

Knowing that the same d_{est-xy} can be calculated using different (x, y) coordinates, it is necessary to calculate the average of the different RSS values corresponding to the d_{est-xy}.

For the scenario of positioning, the signals from the four LEDs and their corresponding RSS values can be collected by the receiver in different coverage areas of the transmitter light. Based on the RSS measurements, the horizontal distances between receiver and LEDs can be obtained from Eq. (25).

2.4.1 Position estimation algorithm

When there are a small number of reference points, the most reliable estimation of the receiver location is obtained by using linear least square estimation. Note that the distances from several reference points (horizontal coordinates of transmitters) are known. After calculating the estimated horizontal distance between the receiver and each of the four transmitters (A, B, C, D), a set of four quadratic equations is formed:

$$(x - x_A)^2 + (y - y_A)^2 = d_A^2 \tag{26}$$
$$(x - x_B)^2 + (y - y_B)^2 = d_B^2 \tag{27}$$
$$(x - x_C)^2 + (y - y_C)^2 = d_C^2 \tag{28}$$
$$(x - x_D)^2 + (y - y_D)^2 = d_D^2 \tag{29}$$

where x_A, x_B, x_C, x_D and y_A, y_B, y_C, y_D are the coordinates of LEDs in X and Y axes, d_A, d_B, d_C, d_D are the horizontal distances from the receiver to LED bulbs, and (x, y) is the receiver position to be estimated.

For a considerable number of estimated locations, we calculate the average and make an approximation in order to find the coordinates of the estimated receiver position.

For three dimensional spaces the receiver position is noted (x, y, z) and the four quadratic equations become:

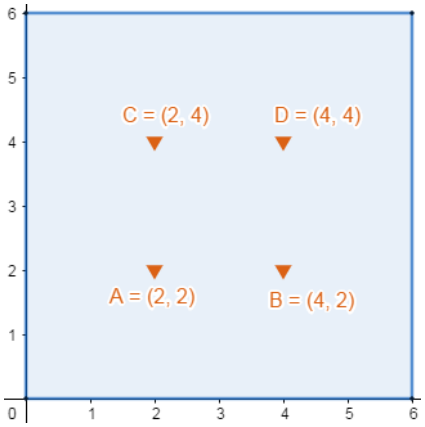

Fig.4: *LED arrangements for different coordinates.*

$$(x - x_A)^2 + (y - y_A)^2 + (z - z_A)^2 = d_A^2 \quad (30)$$

$$(x - x_B)^2 + (y - y_B)^2 + (z - z_B)^2 = d_B^2 \quad (31)$$

$$(x - x_C)^2 + (y - y_C)^2 + (z - z_C)^2 = d_C^2 \quad (32)$$

$$(x - x_D)^2 + (y - y_D)^2 + (z - z_D)^2 = d_D^2 \quad (33)$$

In our case, users are concerned about two-dimensional (2-D) locations.

2.5 Simulation Model

The simulation model is based on the following parameters: the office room size is 6 m × 6 m × 4 m, the LEDs are installed on the ceiling, the height of desk is 1 m, and the receiver is placed on the working plane. The other simulation parameters are listed in Tables 1, 2, and 3.

The four LEDs are respectively located at (2, 2, 4), (4, 2, 4), (2, 4, 4), and (4, 4, 4) in the ceiling as shown in Fig. 4. They perform as a single optical transmitter. To distinguish the light signal power from each LED lamp, the TDM technique is used. In the case that move than four LEDs exist, the brightest four LEDs are selected. The LED lamps radiate their light in assigned time slot. That is, [1 0 0 0], [0 1 0 0], [0 0 1 0], and [0 0 0 1] are transmitted by LED-A, LED-B, LED-C, and LED-D, respectively.

3. RESULTS AND DISCUSSION

In order to study the impact of ambient light on positioning accuracy, different criteria are evaluated.

3.1 Illuminance Performance

From Eqs. (11) and (12), the luminance intensity of an LED changes according to the transmission distance and the angle transmitter/receiver, which these parameters deliver the signal features. Generally, the strength of the received signal is proportional to luminance intensity. There is a nonlinear feature

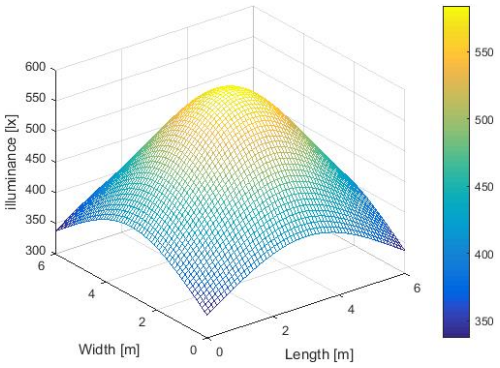

Fig.5: *Distribution of illuminance with one transmitter max value = 584 lx.*

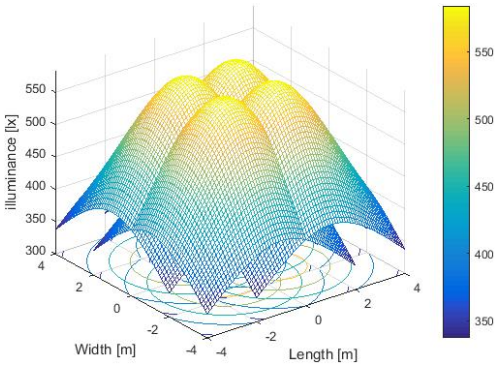

Fig.6: *Distribution of illuminance of four transmitters max value = 584 lx, min value = 337.1726 lx, average = 460.7170 lx.*

of illumination according to distance and angle. A specific position using the change in received signal characteristics can be found [2]. The distribution of illuminance of this system with one transmitter is shown in Fig. 5. The maximum value of luminous flux in the center (3, 3) is 584 lx. Fig. 6 shows the distribution for four transmitters where the value ranges from 337.1726 to 584 lx. The average value is 460.7170 lx.

According to the International Organization for Standardization (ISO), the illuminance of this system is from 300 to 1500 lx, which is sufficient for office work.

3.2 Evaluation of SNR

In this section, the influence of noise on the system performance is studied. First, the case where the channels are all LOS is considered. The distribution of SNR for the LED-D is represented in Figs. 7 and 8. From this, the effects of the increased contribution from shot noise to the total noise is observed, which resulted in a decrease of 10 dB in the direct sunlight exposure compared with indirect exposure in a room environment for the same location.

From both figures, one can see that in the room

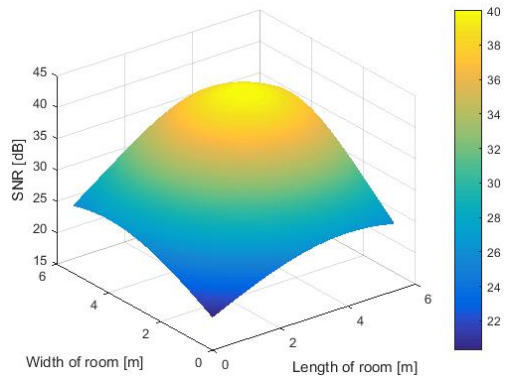

Fig.7: *SNR distribution for LED-D considering LOS channel (direct sunlight exposure).*

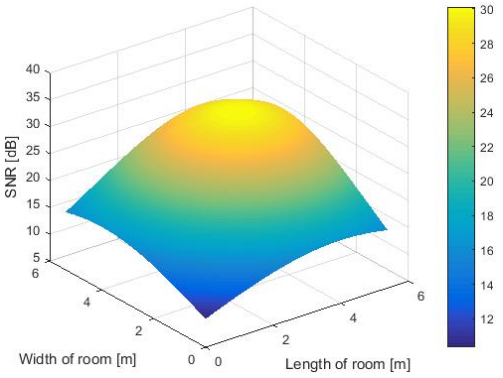

Fig.9: *SNR distribution for LED-D considering NLOS channel (direct sunlight exposure).*

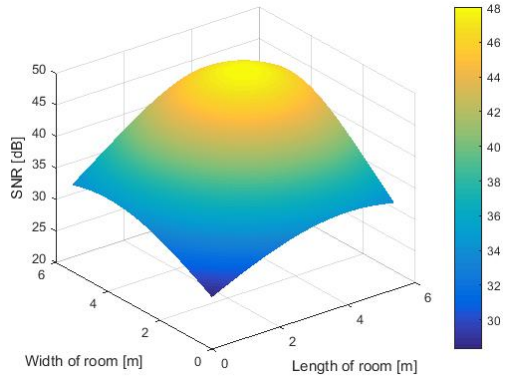

Fig.8: *SNR distribution for LED-D considering LOS channel (indirect sunlight exposure).*

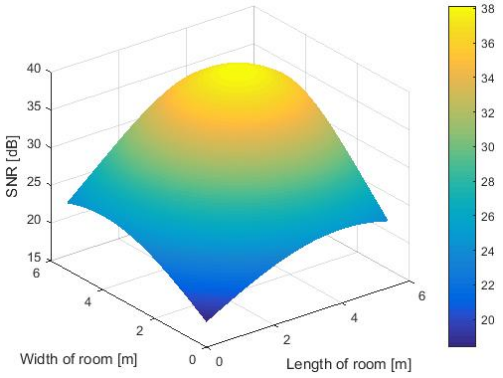

Fig.10: *SNR distribution for LED-D considering NLOS channel (indirect sunlight exposure).*

corner, the transmitted signal has a very low SNR. This leads to relatively large error in estimating of distance in the case where the receiver is located in the corner. Of course the performance of the system decreases when the distance between the LEDs and the receiver increases.

Secondly, we take into account the diffuse channel. Figs. 9 and 10 show that the SNR is decreased by a value of about 10 dB compared to the results obtained by considering the channels all to be LOS. This is due to path loss effect. The SNR in direct sunlight exposure is lower than indirect sunlight exposure by about 8 dB which results in a low signal. This affects the accuracy of the system determination of locations.

3.3 Different Estimated Positions

The distance value is easily obtained by detecting the RSS information of received data coming at each time slot and using Eqs. (26) – (29). Fig. 11 shows the results of trilateration at (5, 5).

Assuming that the position of the receiver is at (5, 5), five average distances estimations are obtained, hence five estimated positions. By calculating their average, we approximate x and y. Taking the orientation angle of the receiver into consideration

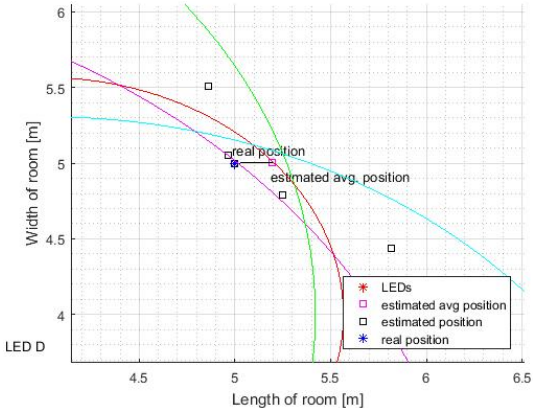

Fig.11: *Zoom view in results of trilateration at (5, 5) (near of the corner).*

we get coordinates (5.195, 5.004) as the estimated receiver position. An error of 19.46 cm (near of the corner) is obtained. When the position of the receiver is at (3, 3), the coordinates (2.983, 3.011) are obtained. This point is considered as an estimated of the receiver position. An error of (1.992 cm) is observed as one can see in Fig. 12.

Fig. 13 presents 61 points on the bottom XY-plan, where the average location error calculated is 2.8 cm.

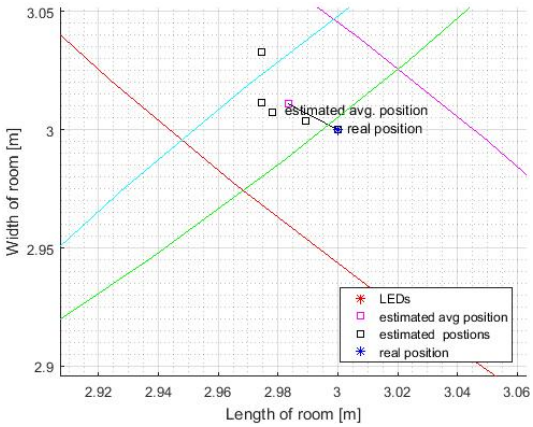

Fig.12: *Zoom view in results of trilateration at (3, 3) (at the centre).*

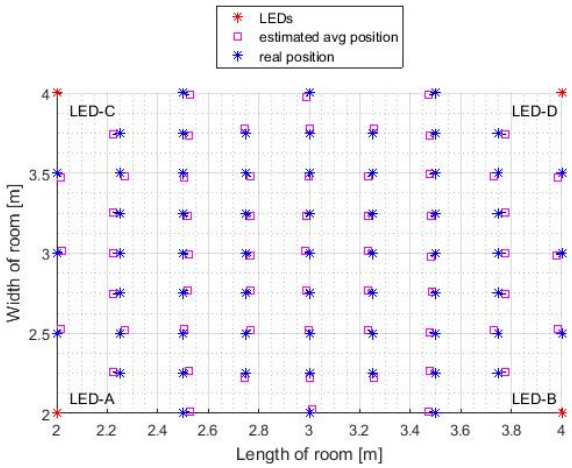

Fig.13: *61 different real positions and estimated positions.*

The location error is mainly caused by additive white Gaussian noise. It is worse in the corners. It is caused by a weakening of the signal from the LED lamp due to the reflection. So, when we move away from the centre, the location error increases.

To determine the position, the selection of four lights far away from walls seems to be a good solution in cases requiring a considerable number of lights. Generally, the lights for illumination are located far away from walls, which decreases the noise creates by the reflected light.

The effects of the walls have a very important impact on the accuracy of positioning.

For the LOS channels, the error is about 1 cm [8]. For the NLOS channels (which are closer to real situations), the average positioning error is about 2.8 cm.

Fig. 14 shows the positioning error distribution in the presence of indirect sunlight exposure. Fig. 15 depicts the result when direct sunlight exposure is assumed.

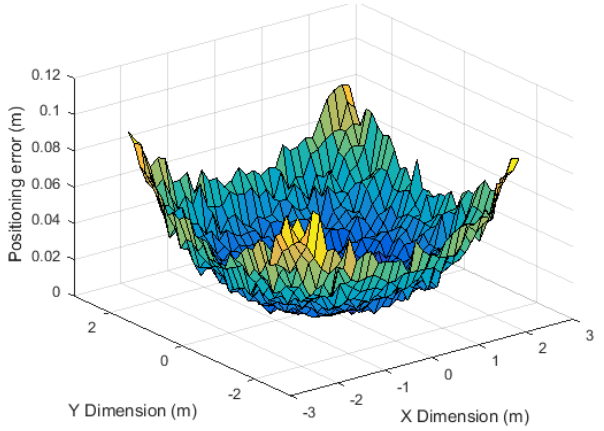

Fig.14: *Positioning error distribution (indirect sunlight exposure).*

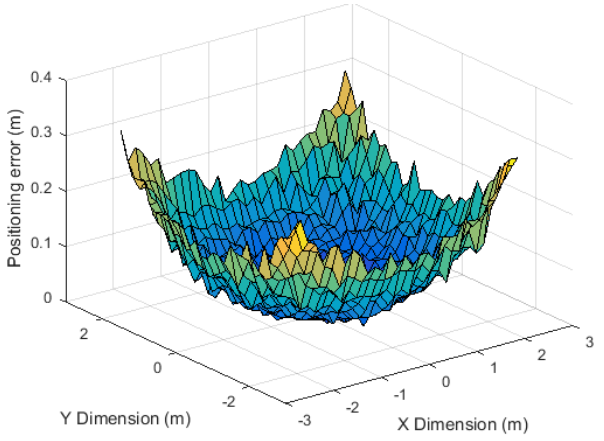

Fig.15: *Positioning error distribution (direct sunlight exposure).*

As expected, the positioning errors are relatively small for the majority of the room, but become much larger when the receiver is close to the corners. Moreover, the positioning error obtained with indirect sunlight exposure (2.88 cm) is much smaller compared to the situation of direct sunlight exposure (9.68 cm) which is a more noisy environment. To directly compare the difference between these two scenarios, the positioning error histograms are shown in Figs. 16 and 17.

To assess the performance of a positioning system more practically, precision is an important evaluation criterion. Generally, the cumulative distribution function (CDF) of positioning error is used to evaluate the precision. The CDF curves of this system are illustrated in Fig. 18.

For direct sunlight exposure, the results show that the service coverage rate is 92%. In this case the proposed system is able to deliver an accuracy of 9.68 cm. For the case of indirect sunlight exposure with the same coverage rate (92%), the system is able to give an accuracy of 2.88 cm.

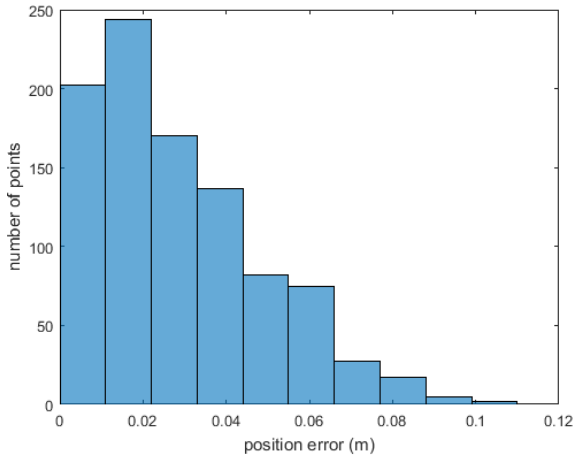

Fig.16: *Histogram of positioning error (indirect sunlight exposure).*

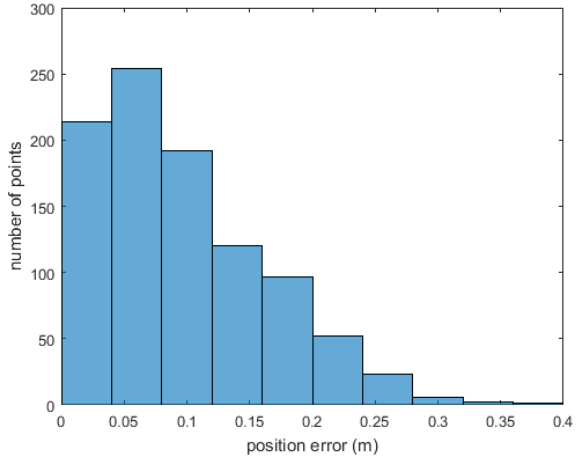

Fig.17: *Histogram of positioning error (direct sunlight exposure).*

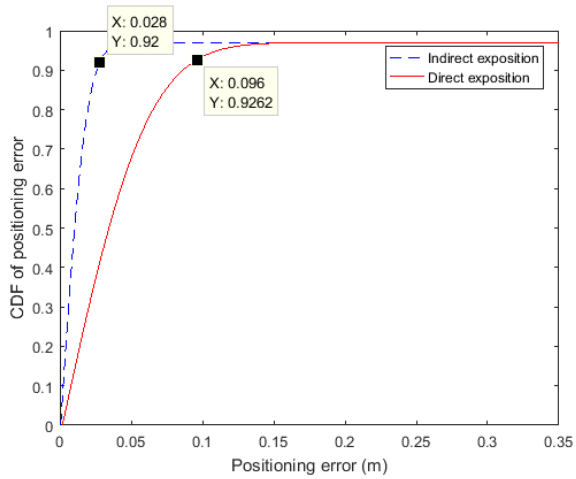

Fig.18: *Cumulative distribution function (CDF) curves of positioning error (direct and indirect sunlight exposure).*

4. CONCLUSION

This paper studied the impact of ambient light on position accuracy for an indoor visible light positioning system. The simulation of the model is carried out by using the trilateration technique. The study explores both cases considering the effects of wall reflection, and cases neglecting them.

This analysis takes into consideration several aspects: wall reflections, direct and indirect sunlight exposure and also the orientation angle of receiver. The simulation program provides the distribution of illuminance, the analysis of SNR, and the positioning error distribution. A 2.8 cm average positioning error is achieved.

In this work, the receiver studied is in a static state. In most applications, the localized target is mobile (robots, people etc.). It would be interesting to study dynamic cases, for example tracing movement trajectory in real time.

ACKNOWLEDGEMENT

This work was supported by the Ministry of Higher Education and Scientific Research of Algeria.

References

[1] Y. Y. Won, S. H. Yang, D. H. Kim and S. K. Han, "Three-dimensional optical wireless indoor positioning system using location code map based on power distribution of visible light emitting diode," *IET Optoelectronics*, vol. 7, no. 3, pp. 77–83, 2013.

[2] S. H. Yang, D. R. Kim, H. S. Kim, Y. H. Son and S. K. Han, "Indoor positioning system based on visible light using location code," in *Proceedings of Communications and Electronics (ICCE)*, pp. 360–363, 2012.

[3] A. L. Pak, A. Rastegarnia, A. Khalil and Md. K. Islam, "A Distributed Target Localization Algorithm for Mobile Adaptive Networks," *ECTI Transactions on Electrical Engineering, Electronics, and Communications*, vol. 14, no. 2, pp. 47–56, August 2016.

[4] L. Shi *et al.*, "5G Internet of Radio Light Positioning System for Indoor Broadcasting Service," *IEEE Transactions on Broadcasting*, vol. 66, no. 2, pp. 534–544, June 2020.

[5] Z. Zhou, M. Kavehrad and P. Denga, "Indoor positioning algorithm using light-emitting diode visible light communications," *Optical Engineering*, vol. 51, no. 8, 085009, 2012.

[6] N. Ul-Hassan, A. Naeem, M. Adeel Pasha, T. Jadoon and C. Yuen, "Indoor Positioning Using Visible LED Lights: A Survey," *ACM Computing Surveys*, vol. 48, No. 2, Article 20, 2015.

[7] L. Grobe *et al.*, "High-speed visible light com-

munication systems," *IEEE Communications Magazine*, vol. 51, no. 12, pp. 60–66, 2013.

[8] X. Huang, Y. Wang, Y. Wang, C. Yang, J. Li and N. Chi, "Experimental demonstration for high speed integrated visible light communication and multimode fiber communication system," *IET Optoelectronics*, vol. 9, no. 5, pp. 207–210, 2015.

[9] W. Zhang, M. I. S. Chowdhury and M. Kavehrad, "Asynchronous indoor positioning system based on visible light communications," *Optical Engineering*, vol. 53, no. 4, 045105, 2014.

[10] L. Wang, C. Wang, X. Chi, L. Zhao and X. Dong, "Optimizing SNR for indoor visible light communication via selecting communicating LEDs," *Optics communications*, vol. 387, pp. 174–181, 2017.

[11] D. O'Brien *et al.*, "Indoor Visible Light Communications: challenges and prospects," *Proceeding of SPIE*, vol. 7091, 709106, 2008.

[12] A. Chaabna, A. Babouri and X. Zhang, "An Indoor Positioning System Based on Visible Light Communication Using a Solar Cell as Receiver," in *Artificial Intelligence in Renewable Energetic Systems, Lecture Notes in Networks and Systems, vol. 35*, M. Hatti, Ed., Springer, 2018, pp.43–49.

[13] V. Jungnickel, V. Pohl, S. Nonning and C. Von Helmolt, "A Physical Model of the Wireless Infrared Communication Channel," *IEEE Journal on Selected Areas in Communications*, vol. 20, no. 3, pp. 631–640, 2002.

[14] M. Karppinen *et al.*, "Wireless infrared data links: ray-trace simulations of diffuse channels and demonstration of diffractive element for multibeam transmitters," *Optical Engineering*, vol. 41, no. 4, pp. 899–910, 2002.

[15] J. Panta, P. Saengudomlert and K. Sripimanwat, "Performance Improvement of ACO-OFDM Indoor Optical Wireless Transmissions Using Partial Pre-Equalization," *ECTI Transactions on Electrical Engineering, Electronics, and Communications*, vol. 14, no. 1, pp. 1–11, February 2016.

[16] J. M. Kahn and J. R. Barry, "Wireless infrared communications," *Proceedings of IEEE*, vol. 85, no. 2, pp. 265–298, 1997.

[17] A. Sivabalan and J. John, "Improved power distribution in diffuse Indoor Optical Wireless systems employing multiple transmitter configurations," *Optical and Quantum Electronics*, vol. 38, pp. 711–725, 2006.

[18] T. Komine and M. Nakagawa, "Fundamental analysis for visible-light communication system using LED lights," *IEEE Transactions on Consumer Electronics*, vol. 50, no. 1, pp. 100–107, 2004.

[19] A. J. Moreira, R. T. Valadas, and A. M. de Oliveira Duarte, "Optical interference produced by artificial light," *Wireless Networks*, vol. 3, no. 2, pp. 131–140, 2004.

[20] R. G. Smith and S. D. Personick, "Receiver design for optical fiber communication systems," in *Semiconductor Devices for Optical Communication, Topics in Applied Physics, vol. 39*, H. Kressel, Ed., Springer, 1982, pp. 89–160.

[21] G. Archenhold, "Health and safety of artificial lighting," *Mondo Arc*, vol. 63, pp. 111–118, 2011.

[22] Z. Guo, Z. Jia, W. Xia, Y. Zhang and L. Shen, "Indoor Localization System for Mobile Target Tracking based on Visible Light Communication," in *Proceeding of 2017 IEEE 85th Vehicular Technology Conference (VTC Spring)*, 2017, pp. 1–5.

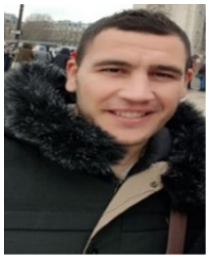

Ameur Chaabna received his Master degree in automatic from the University Kasdi Merbah Ouargla, Algeria in 2015. He received a doctorate degree in Electronic from the University of Guelma, Algeria. He is a member of the LABCAV Laboratory. His current research interests include visible light communication (VLC), indoor localization, positioning algorithm, positioning performance, energy efficiency and spectral compression.

Abdesselam Babouri received the Ph.D. in Electronic from the University of Lorraine Nancy, Lorraine, France in 2007. He is currently a Full professor in Department of Electrical and Automatic Engineering at the University of 8 Mai 1945 Guelma, Algeria, and a team Leader of electromagnetic compatibility and biomedical systems at the LGEG Laboratory. He has authored more than 60 papers in international journal or conference proceedings. His main research interests are sensor networks and biomedical application, visible light communication (VLC), clinical evaluation of pacemaker systems and electromagnetic compatibility.

Xun Zhang received his B.Eng from Wuhan University of technology, an M.E. degree from Université Marrie Pierre Curie in 2005, and Ph.D. from Nancy University in 2009. He obtained a Post-Doc fellowship of Motorola Foundation in IETR/SCEE at Supélec in 2010. He is currently employed as an associate professor in MINARC team of laboratory at the Institut Supérieur d'Électronique de Paris (ISEP). His research activities involve algorithm implementation optimization for Visible Light Communication (VLC) and Feedback Systems Control for sleep apnea. Dr. Zhang has published more than 30 peer-reviewed journal and conference papers.

Fayçal Boulsina received the Ph.D. in Electronics from Constantine University, Algeria, in 2009. Since 2009, he has been a Lecturer with Guelma University, Algeria. His main research interests are improving the depth resolution of secondary ion mass spectrometry (SIMS) by deconvolution, characterization of semiconductor materials, and signal processing.

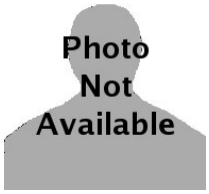

Takoua Hafsi received her Master degree in scientific calculation from the University Badji Mokhtar Annaba, Algeria in 2012. She received a doctorate degree in Mathematics from the University of Badji Mokhtar Annaba, Algeria. She is a member of the Mathematical Modelization and Numerical Simulation Laboratory (LAM2SIN). Her current research interests include contact problems, analysis , modeling and simulation.